LBNL-42375

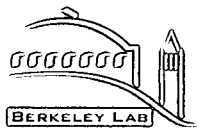

ERNEST ORLANDO LAWRENCE
BERKELEY NATIONAL LABORATORY

Subsurface Electromagnetic Measurement through Steel Casing

Alex Becker, Bing Wang, Ki Ha Lee, and Mike Wilt

Earth Sciences Division

November 1998

LBNL-42375

Subsurface Electromagnetic Measurement through Steel Casing

by
Alex Becker
Bing Wang
Ki Ha Lee
Ernest Orlando Lawrence Berkeley National Laboratory

and

Mike Wilt
Lawrence Livermore National Laboratory

November 1998

This study was supported in part by the Assistant Secretary for Fossil Energy, Office of Gas and Petroleum Technologies of the U.S. Department of Energy under Contract No. DE-AC03-76SF00098.

Subsurface Electromagnetic Measurement through Steel Casing

Abstract

Numerical calculations show that useful information can be obtained in an electromagnetic crosswell survey where one of the wells is cased in steel. Our simple model is based on the assumption of an infinitely long uniform casing embedded in a homogenous full space. Nevertheless the results indicate that if the pipe characteristics are independently known then the formation signal can be accurately recovered. This is best done at a single frequency where the pipe attenuation is modest. In fact we show that the optimal frequency for formation signal recovery is defined mainly by the pipe parameters and is largely independent of the formation conductivity.

Introduction

This feasibility study of subsurface electromagnetic measurements is a direct outgrowth of our previous work in fiber cased wells. As previously reported by Wilt et al (1995), we demonstrated the practicality and utility of interwell measurements on an oil field scale, at Devine, TX and at Lost Hills, CA. On a smaller scale, we carried out a demonstration of interwell and surface to borehole EM tomography with controlled experiments at the University of California Richmond Field Station. Since virtually all oil wells are cased in steel, it is natural that our studies on interwell electromagnetic measurements be extended to situations where at least one well is cased in steel.

Results of previous theoretical work and numerical calculations by Augustin et al (1989), Uchida et al. (1991) and Wu and Habashy (1994) all pointed to the possibility of extracting a formation signal from electromagnetic measurements through casing. In particular, the Augustin results showed that the casing acts as a strong low pass filter. The Wu paper demonstrated further that the signal attenuation process in the casing resembles the attenuation of a plane wave in a conductive medium where the controlling factor is the ratio of the distance traveled to the skin depth. Neither of these two studies was done for the crosswell configuration and their results needed to be re-examined. Finally we note that while Uchida et al. suggested that interwell EM tomography was feasible they also indicated that the casing attenuation factor was to some degree a function of the position of any external source. This last feature of signal transmission through casing was seen as a possible difficulty in interpreting the filtered signals.

In this report, which was circulated to the research sponsors in draft form some time ago, we provide an overview of the signal attenuation process and verify the recovery of the original reservoir formation signal from its observable attenuated and phase shifted form. Using numerical calculations we show that useful information can be obtained in an electromagnetic crosswell survey where one of the wells is cased in steel. Our simple model is based on the assumption of an infinitely long uniform casing embedded in a homogenous full space. Nevertheless the results indicate that if the pipe characteristics are known independently, then the

formation signal can be accurately recovered. This is best done at a frequency where the pipe attenuation is modest. In fact we show that the optimal frequency for formation signal recovery is defined mainly by the pipe parameters and is largely independent of the formation conductivity.

Numerical Computations

Code Description

The data required for this study were generated with the "Cas4" computer program which is described in a companion LBNL report (Song and Lee, 1998). It is based on an analytical solution for a cylindrically symmetric source and medium boundaries. The evaluation of the resultant integrals is done numerically. The computational parameters for an "infinitely long" pipe are illustrated in Figure 1. Here we have three regions for which the dimensions, the magnetic permeability and the electric conductivity can be specified. The first region lies within the casing and contains a single turn source loop of radius "a" that carries a one ampere current. The dimension of this region is defined by the inner casing radius "b" and the electrical conductivity is that of the drilling mud. The second region corresponds to the casing itself and is defined by the casing outer radius "c" and the magnetic permeability μ_2 and electrical conductivity σ_2. The formation, defined by its conductivity σ_3 constitutes the third region which also contains the receiver. The positioning of the transmitter within the casing is a computational requirement. In practice, it is the receiver that would occupy that place. The problem symmetry however guarantees that these two elements are electromagnetically reciprocal and can be interchanged for computational purposes.

Code Verification

Although the experimental results presented by Augustin et al. (1981) already confirmed the validity of the "Cas4i" code, it was thought prudent to repeat the code verification for the source-receiver configuration of interest here. The tests were done in the laboratory on a 2.5 m length of common 3" OD iron pipe. Approximate measurements of the pipe parameters indicated a relative magnetic permeability of about 120 and an electrical conductivity of about 10^7 S/m. The pipe had an inner radius of 3.2 cm and a 0.5cm wall thickness. The experimental arrangement is shown in Figure 2. The transmitter loop had an effective area of 0.53 m^2 and carried a current of about 2 A. The receiver was a Develco 9200C fluxgate magnetometer with a narrow band sensitivity better than 0.3 nT and a cut-off frequency well above the 10 ~ 500 Hz measurement range. The receiver and transmitter were coplanar and separated by a distance of 40 cm.

The experimental attenuation and phase shift data for the test pipe are shown in Figure 3, where they are compared to the corresponding theoretical values generated with the numerical code. Both the amplitude data in decibels (dB) and the phase data in degrees are plotted against the square root of the measurement frequency so as to demonstrate the linearity of the phase and the exponential dependence of the attenuation of the amplitude on that experimental parameter. Here again we have an independent verification of the observation made by Wu et al. (1994) that the filtering of the signal by the casing is largely determined by single induction parameter defined by the ratio of casing thickness to the skin depth in the metal. The accuracy of the laboratory

measurements, which were made with rudimentary equipment, is estimated to be about ± 5% in amplitude and about ± 5° in phase. Within this accuracy, good agreement is observed between the experimental and numerical data, confirming the validity of the "Cas4" code.

A further single frequency test of the code involved a transmitter traverse outside the pipe. The traverse was parallel to the pipe axis at 40 cm radial distance from the receiver which was stationary within the pipe. The transmitter and receiver axes were parallel to the pipe length. The results for this test that was done at 100 Hz, are shown in Figure 4. Once again, within the limits of experimental error, we see good agreement between numerical and experimental data. More importantly however, we note that the shape of the field strength variation is very similar to that which would be observed in free space.

Numerical Results

Attenuation and Phase Shift Characteristics

Most of our numerical investigations were dedicated to a study of the casing transfer function for a receiver-transmitter system with axes parallel to the casing axis. After many trial variations in the casing parameters, formation conductivity and system geometry, we concluded that the key variable was the casing induction number (t / δ) and, to a much lesser degree the relative position of the transmitter and receiver. Typical data for a common casing size and a coplanar receiver-transmitter are shown in Figure 5. Here we have a coplanar system with a 100 meter receiver-transmitter separation. The inner casing radius is 10 cm, the thickness is 1 cm, the relative magnetic permeability is 100 and the electrical conductivity is 2×10^6 S/m. For comparison purposes, we show, on the same scales, the free space pipe transfer function and the filtered formation signal for a 0.1 S/m formation conductivity. As we have observed previously, the casing attenuation factor expressed in dB and the casing induced phase shift vary linearly with the casing induction parameter. The effect of the formation appears at a casing induction parameter value of 2.5 which corresponds to a frequency of about 20 Hz. As expected, the presence of the formation affects the attenuation and phase shift of the observed signal.

The spatial variation in the casing attenuation and phase shift characteristics was investigated previously by Uchida et al. Our findings for the free space effects of the casing used in the previous example, at 300 Hz, are presented in Figures 6 and 7. The results confirm the Uchida data which also showed that the casing attenuation and phase shift characteristics exhibited spatial variability for small coil separation when one of the system elements is positioned in the vicinity of the cased well.

In our example, the average casing attenuation factor is about 38.6 dB and varies by no more than about ± 1 dB or ± 12 % throughout the region of interest. The predominant phase shift is about 65°, but this can rise to nearly 90° or fall below 50° in regions very close to the source.

Recovery of formation signal

It is our contention that the formation signal can be recovered if the transfer function for the casing is known. To demonstrate this point, let us again consider the data shown in Figure 5. If the proposition is true, then one can simply obtain the formation signal by taking the formation plus casing data, and correcting it for the attenuation and phase shift attributable to the casing. The phase correction simply involves a subtraction of the "free space" casing related phase shift from the simulated "observed" phase shift for the casing in the formation. Similiarly, the formation signal is obtained by taking the "observed" casing in formation signal and dividing it by the casing attenuation factor for the primary, "free space" field.

We illustrate this procedure for the quadrature component of the formation signal (secondary field) for the parameters used to compute the data shown in Figure 5. If the filtered formation signal is labeled,

$$FFS = Ae^{i\phi}$$

and the casing transfer function is denoted by;

$$CT = Be^{i\varphi}$$

Then the recovered formation signal will be given by;

$$RFS = (A / B)e^{i(\phi-\varphi)}$$

and its quadrature component by,

$$QFS = (A / B)\sin(\phi - \varphi)$$

The results for this computation are shown in Figure 8 where the recovered formation signal is compared to its analytical values. Although the coarseness of the scales does not make this apparent, a closer inspection would reveal that the formation signal phase and amplitude are recovered to better than a few millidegrees and 1%. The results for a similar comparison as a function of system geometry but at a single frequency of 300 Hz are shown in Figures 9 and 10. As before, the calculation is done for system dipoles that are parallel to the pipe axis. In considering the formation signal recovery error for this configuration, we note that they are highest where the observed fields are the weakest. Even then they do not exceed 0.5% in amplitude and 0.25° in phase.

Choice of Optimal Frequency

In the foregoing discussion, we made no distinction between the primary "free space" transmitter field and the secondary field related directly to the eddy currents in the formation. However in order to demonstrate the existence of an optimal frequency range for the proposed interwell measurements through casing, let us consider the eddy current contribution alone. The pertinent data are displayed in Figure 11where we show the attenuation characteristic for our standard test pipe and a coplanar system with a 100m coil separation as well as the secondary field for a 0.25

S/m formation. The observable formation signal is simply the product of the last two quantities. Under the present circumstances, it exhibits a broad peak at about 20 Hz. A more striking presentation of this phenomenon can be made by normalizing the filtered formation signal by the free space transmitter field at the receiver position and plotting the data in log-linear form. This is done in Figure 12 for a number of different formation conductivity values including the 0.25 S/m value considered in the previous illustration. The coplanar configuration and the 100 m spacing is maintained for all four cases.

We note that while the amplitude of the optimal filtered formation signal varies smoothly with the formation conductivity from less than 1% of the free space primary field for the 0.01 S/m formation to more than 10% for the 0.5 S/m formation, the optimal response frequency remains nearly invariant at about 20 Hz. It then appears that the optimal frequency must be a function of the pipe parameter only.

This phenomenon can be qualitatively explained if we admit a number of approximations to the discussion. Assume that the pipe attenuation function is given by:

$$CT = e^{-p},$$

where p is pipe induction parameter which equals to pipe thickness/skindepth in pipe. Further assume that the formation signal is given by:

$$FS = 2q^2,$$

where q is formation induction number and equals to coil separation/skindepth in formation. The filtered signal is then given by

$$FFS = FS * CT = 2q^2 e^{-p}.$$

It can be readily shown that, by introducing a frequency-independent constant

$$c = \left(\frac{r}{t}\right)^2 \frac{\sigma_f}{\mu_r \sigma_p},$$

we have

$$q^2 = cp^2,$$

where r is the coil separation, t is the pipe thickness, μ_r is the relative pipe permeability, σ_f is the formation conductivity, and σ_p is the pipe conductivity. We then have,

$$FFS = 2cp^2 e^{-p}.$$

This function has a well defined maximum at p=2. As observed previously, the corresponding optimal frequency is only a function of pipe parameters and should occur at the point where the pipe exhibits about 14 dB of attenuation.

It must be immediately reiterated that the argument presented above is only as good as the approximations and would lead to an optimal survey frequency of about 50 Hz the stated pipe parameter whereas the numerical data for the parameters used to generate the Figure 11 results indicate an optimal frequency half as big. The answer to this paradox lies in noting that the formation signal shown in Figure 11 rises as $f^{2/3}$ (f is the frequency) instead of f as assumed the argument above. So that

$$FFS = cp^{4/3}e^{-p},$$

with an optimal value of p=4/3. This corresponds to an optimal frequency of about 23 Hz as observed while the actual attenuation in this case is only about 6 dB.

DC magnetic effects in a steel casing

The principal for the formation signal can be recovered if the casing parameters are known. Incidentally, it appears that there is an optimal frequency for doing this that it is primarily determined by the pipe parameters and to a much lesser extent by the induction number in the formation. The successful extension of electromagnetic subsurface measurements to cased borehole depends on one's ability to make an independent possibly contemporary, (with the crosswell survey) estimate of the pipe parameters. We have not really begun to address this issue, but in preparation to do so examined the influence of the casing on DC magnetic fields.

In an exploratory study, we examined the alteration of the magnetic field of a dipole source inside and outside the casing. To do this, we wrote a numerical code based on Kaufman's 1992 analytical solution to the problem. For a dipole of unit moment, the magnetic field component parallel to the pipe when measured externally is given by

$$H_z(r,z) = \frac{1}{2\pi R^3}\int \frac{x^2 K_0(\beta\alpha)\cos(\alpha x)}{1+nx^2 I_0(x)K_0(x)}dx.$$

Here r and z are the radial and axial distance from the source to the observation point, respectively, r_0 is the pipe radius, t is the pipe thickness, μ_r is the relative magnetic permeability of the pipe, and

$$R^2 = r^2 + z^2$$
$$\beta = r / r_0$$
$$\alpha = z / r_0$$
$$n = \mu_r t / r_0$$

In addition, $K_0(.)$ and $I_0(.)$ are modified Bessel functions of the first and second kind of order zero, respectively. Prior to use, we tested the validity of this formulation on a laboratory test pipe which was 8 feet long. Here we had $\mu_r = 120$, t=4.8 mm, and $\sigma_p = 10^7 S/m$. The results of

the test which was quite similar in nature to the AC tests reported previously are shown in Figure 13 for a profile parallel to the pipe and 40 cm separation between source and receiver. For purposes of comparison, we also show the theoretical data generated with the Kaufman solution and the free space dipole field. The analytical and experimental results show good agreement but differ significantly from the field that would be observed in free space. In particular, we note that the source dipole as seen through the casing by an external observer would appear to be at a greater radial distance than it really is. In fact, the distortion of the external, axially directed, field, at DC, is a general phenomenon.

This phenomenon holds beyond the casing. In Figure 14, we display the ratio of the axial component of a dipole field seen through casing to its free space value. Because of the magnetic influence of the casing, the source field is distorted at considerable distances outside the casing. If we compare this data to the attenuation factors shown in Figure 6 however, we note that the primary field distortion is considerably reduced for AC source.

Of greater interest is the axial field along the casing axis. This quantity is given by Kaufman as

$$H_z(z) = \frac{1}{2\pi z^3}\left[1 + n\int \frac{x^4 K_0(\alpha x)}{1 + n^2 x^2 I_0(x) K_0(x)} dx\right],$$

where the symbols retain the meaning assigned to them above.

The results for this calculation for a 6.4 cm diameter pipe as a function of axial distance and the pipe magnetic parameter (n) are shown in Figure 15. Perhaps the most striking feature here is the axial location of the point prior to which the free space field is attenuated and beyond which it is amplified. It appears that the position of this point varies as the fourth root of the magnetic parameter for the pipe. Perhaps this feature can serve as a component of a pipe parameter measurement system.

Conclusions and Recommendations

Our numerical modeling results for crosswell electromagnetic data where one of the wells is cased in steel indicate that the formation signal can be extracted from the field data if the casing parameters are known. In this we agree with previous work on the casing problem done for other transmitter-receiver configurations (Augustin et al., 1989; Wu et al., 1994) where it was shown that the steel casing acts as a linear filter. Although it appears that the casing attenuation function is largely dependent on the casing induction parameter or its thickness/skin depth ratio, the formation signal can only be recovered properly if all the casing parameters are individually known with good accuracy.

We also note that there is an optimum frequency for making EM measurements through casing. At this frequency, the observable formation signal is strongest in absolute terms. However it forms only a relatively small fraction of the total observed signal which also includes the filtered

primary (free space) field. The optimal frequency is uniquely determined by the casing parameters. It occurs where the casing attenuation is relatively mild and equals about 6 dB.

It now appears certain that crosswell em surveys are a reality although much work remains to be done on the measurement of casing properties. We expect that any difficulties in this area can be overcome by the development of a tool specialized for this purpose.

Acknowledgments

Partial funding for this research was provided by a consortium of energy and service companies including the research divisions of Chevron USA Production Company, Japan National Oil Corporation, OYO Corporation, Schlumberger-Doll Research, Texaco, US EPA, Western Atlas Logging Services. Partial funding was also provided by the Assistant Secretary for Fossil Energy, Office of Gas and Petroleum Technology of U.S. Department of Energy under Contract DE-AC03-76SF0098.

References

Augustin, A.M., Kennedy, W.D., Morrison, H.F., and Lee, K. H., 1989, A theoretical study of surface to borehole electromagnetic logging in cased holes: Geophysics, 54, 90-99.

Kaufman, A., 1992, Geophysical field theory and methods, Academic Press.

Song, Y., and Lee, K.H., 1988, Electromagnetic fields due to a loop current in a cased borehole surrounded by uniform whole space, Ernest Orlando Lawrence Berkeley National Laboratory, Report LBNL-42371.

Uchida, T., Lee, K.H., and Wilt, M.J., 1991, Effect of a steel casing on crosshole EM measurement. SEG Expanded Abstracts, EM2.6, 61st Annual International Meeting.

Wilt, M.J., Lee, K.H., Becker, A., Wang, B., and Spies, B., 1996, Crosshole EM in steel-cased boreholes. SEG Expanded Abstracts, EM1.5, 66th Annual International Meeting.

Wilt, M.J., Lee, K.H., Morrison, H.F., Becker, A., Tseng, H.-W., Torres-Verdin, C., and Alumbaugh, D., 1995, Crosshole electromagnetic tomography: A new technology for oil field characterization: The Leading Edge, 173-177.

Wu, X., and Habashy, T.M., 1994, Influence of the steel casings on electromagnetic signals: Geophysics, 59, 378-390.

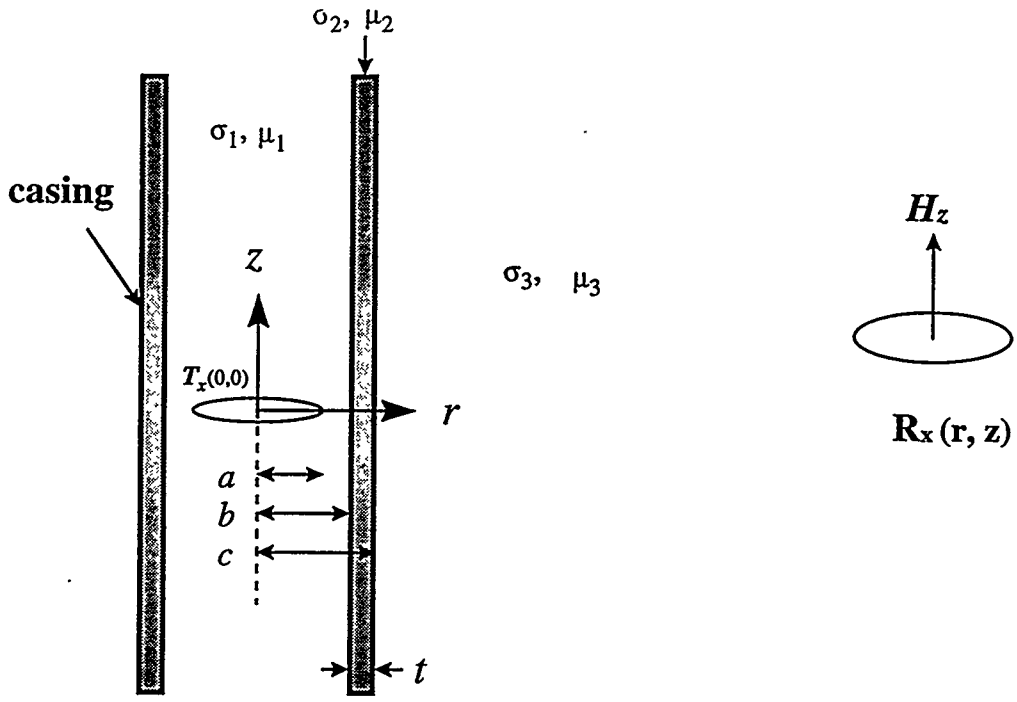

Figure 1. Computational Parameters

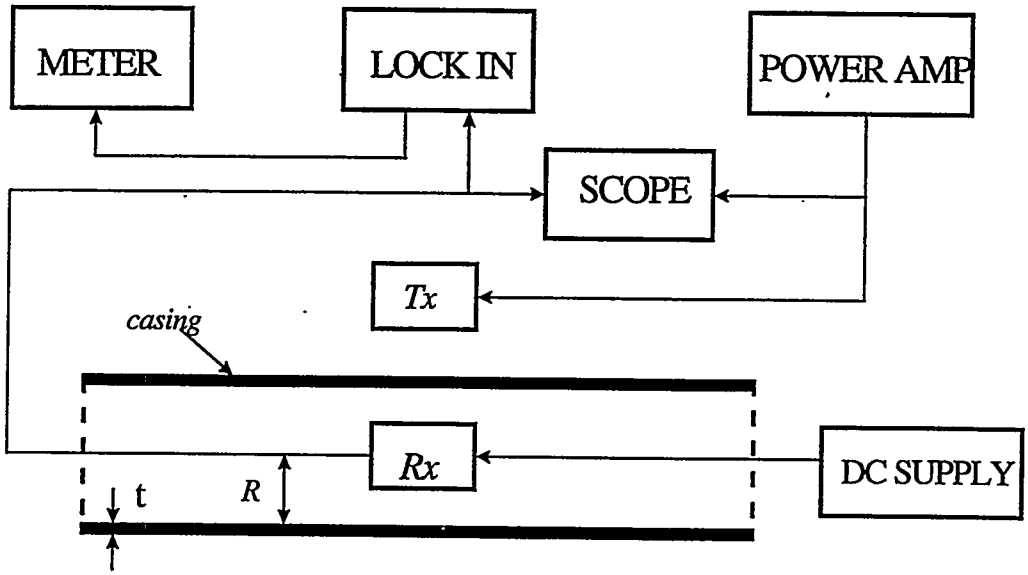

Figure 2. Laboratory Experiment Setup

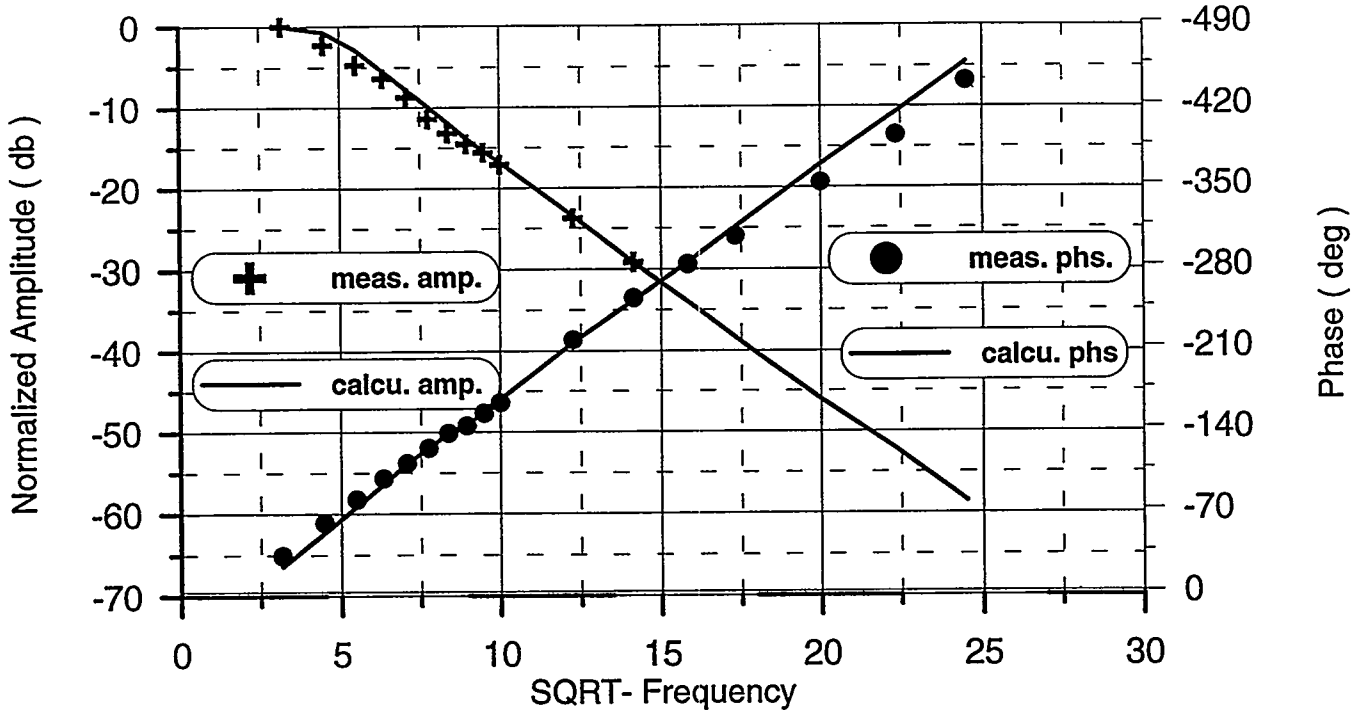

Figure 3. Frequency Response at 40 cm Radial Separation

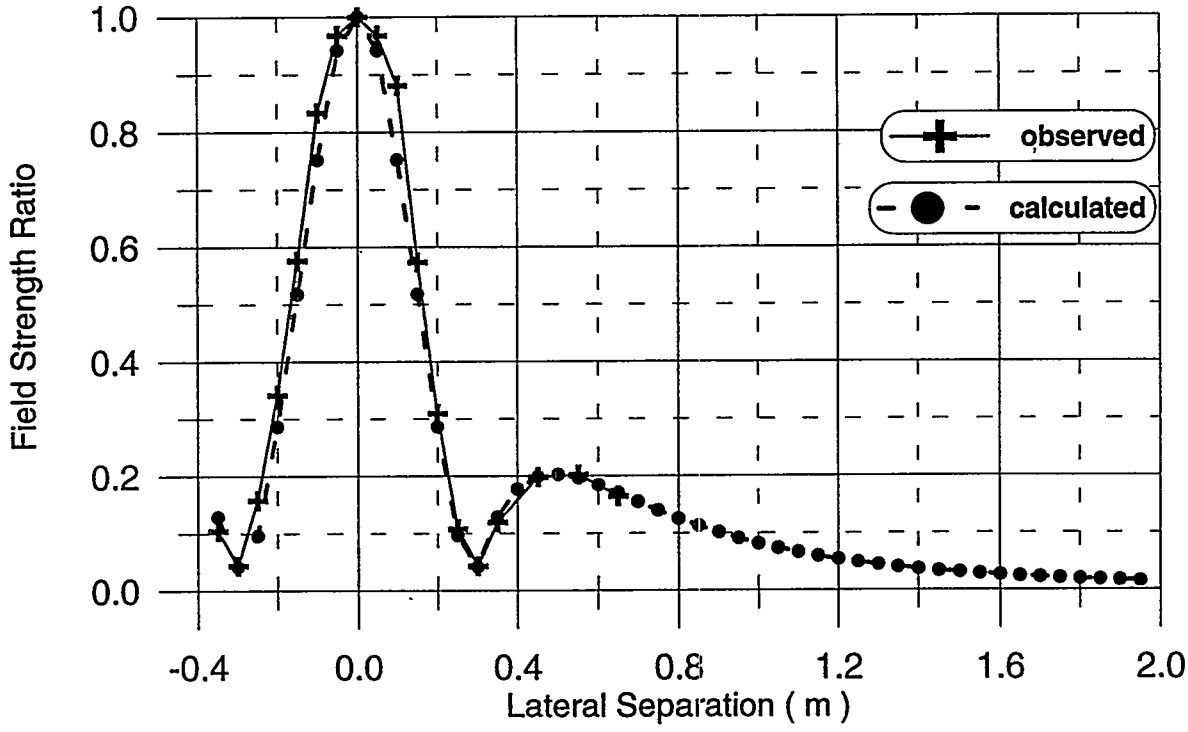

Figure 4. 100 Hz Profile at 40 cm Radial Separation

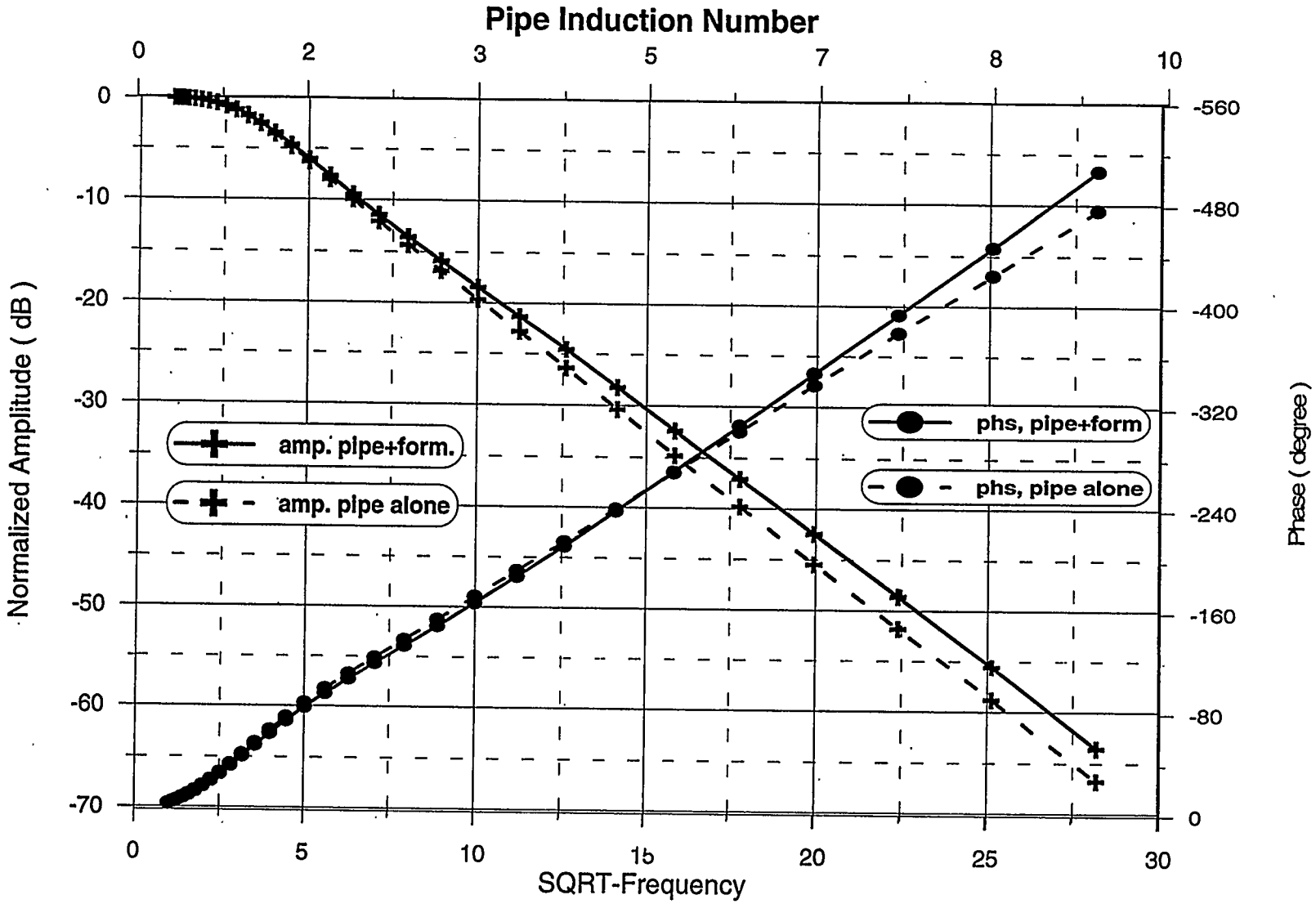

Figure 5. Casing Transfer Function and Formation Signal

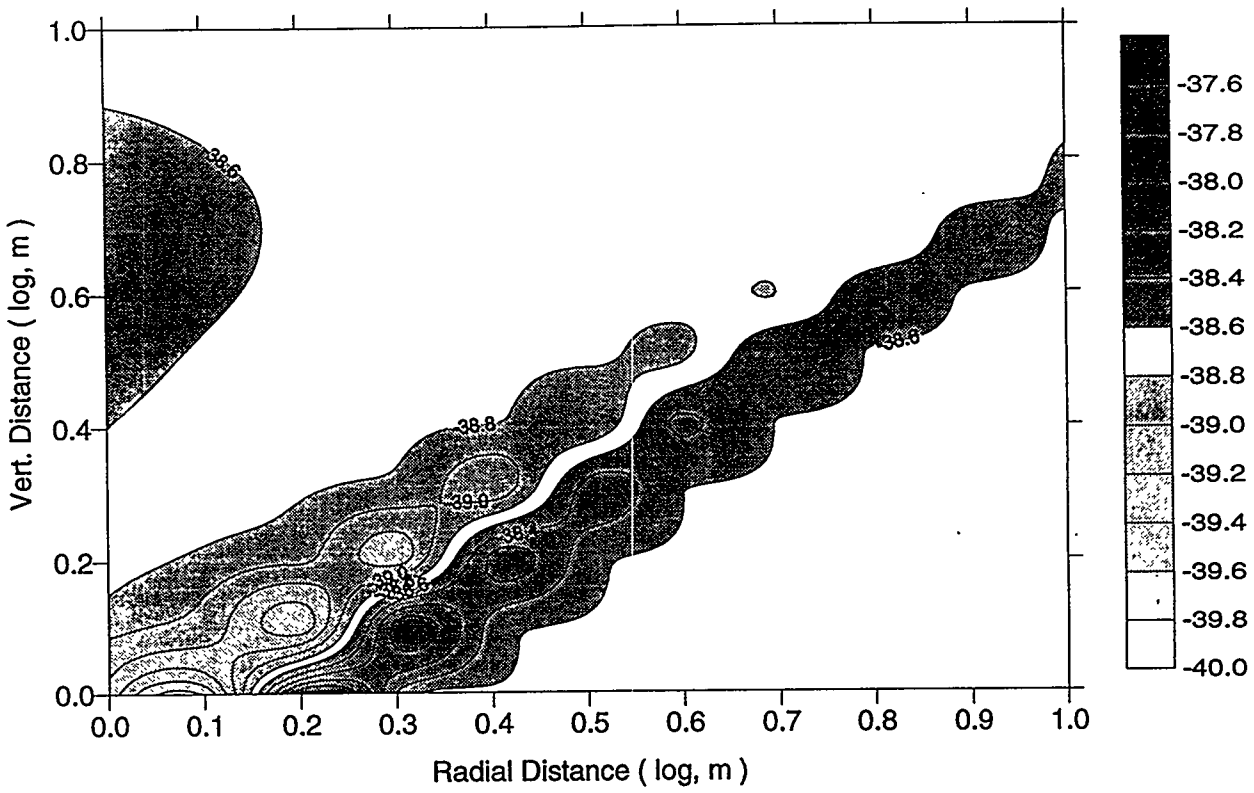

Figure 6. Attenuation at 300 Hz (dB)

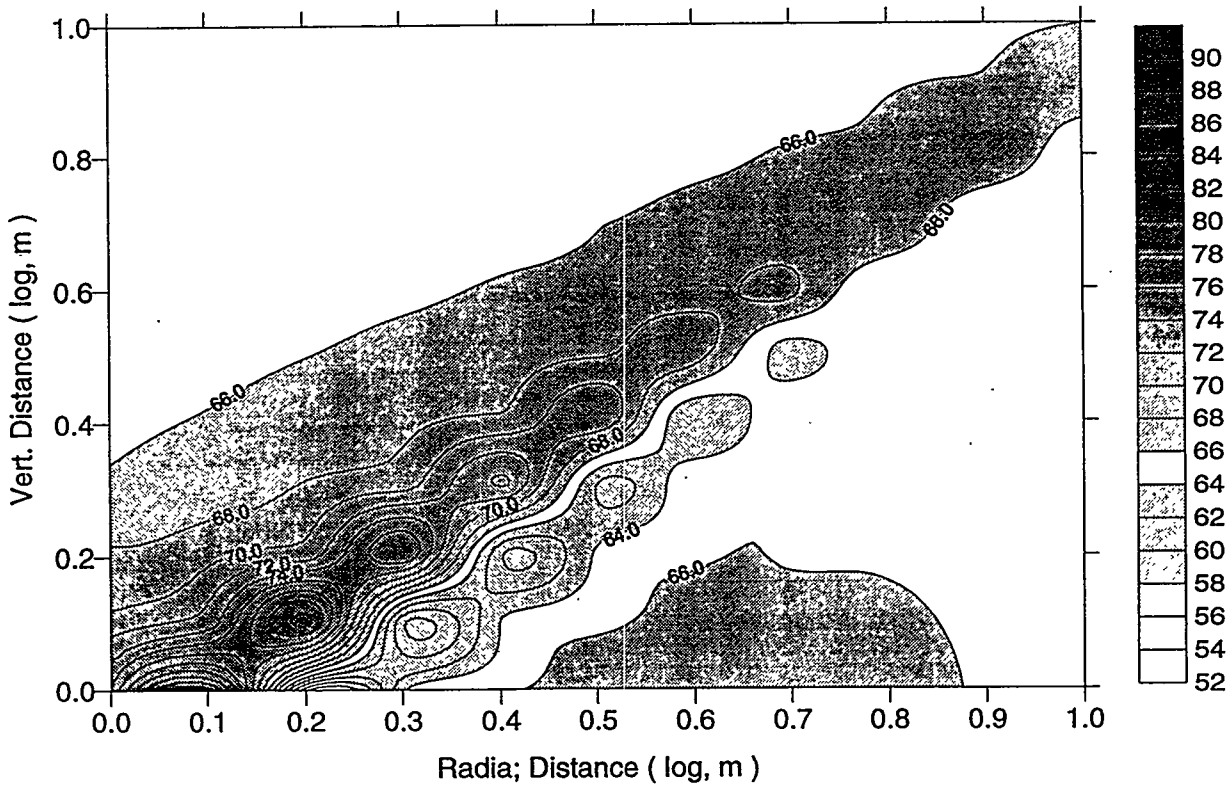

Figure 7. Phase Lag at 300 Hz (degree)

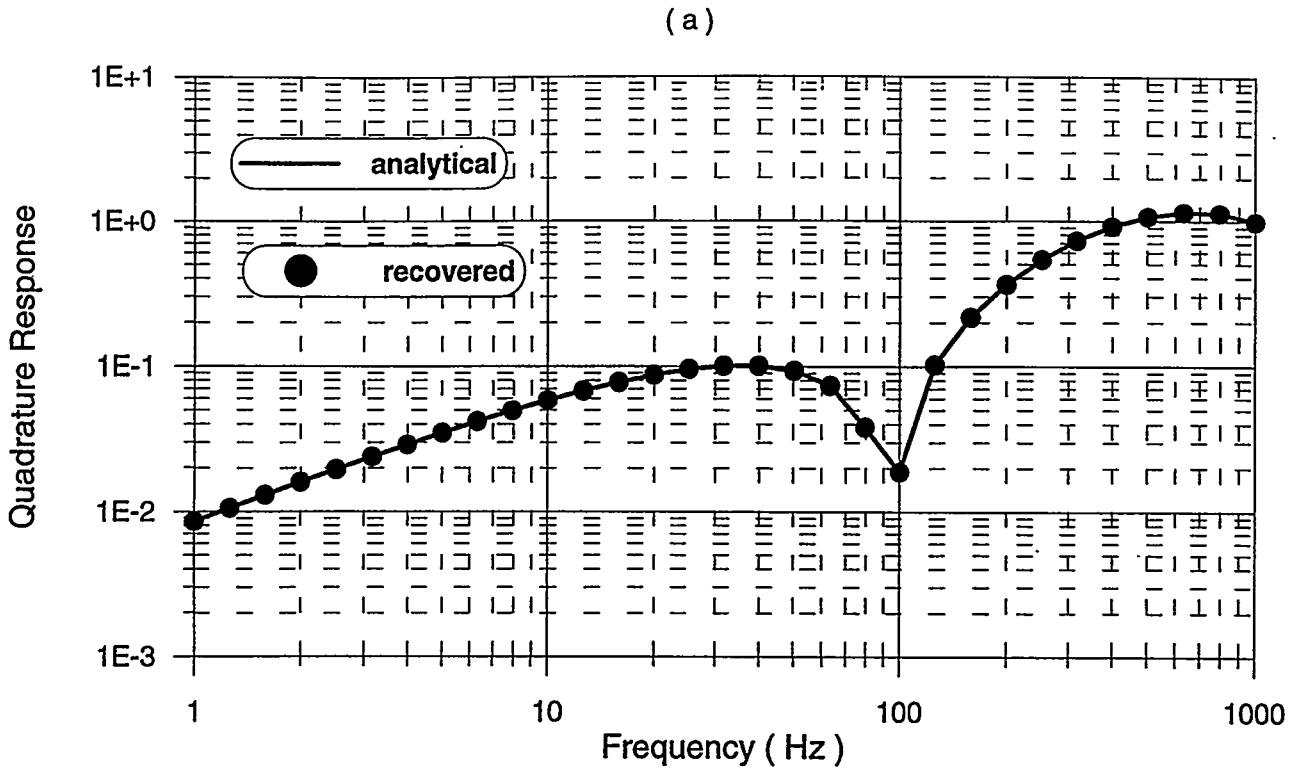

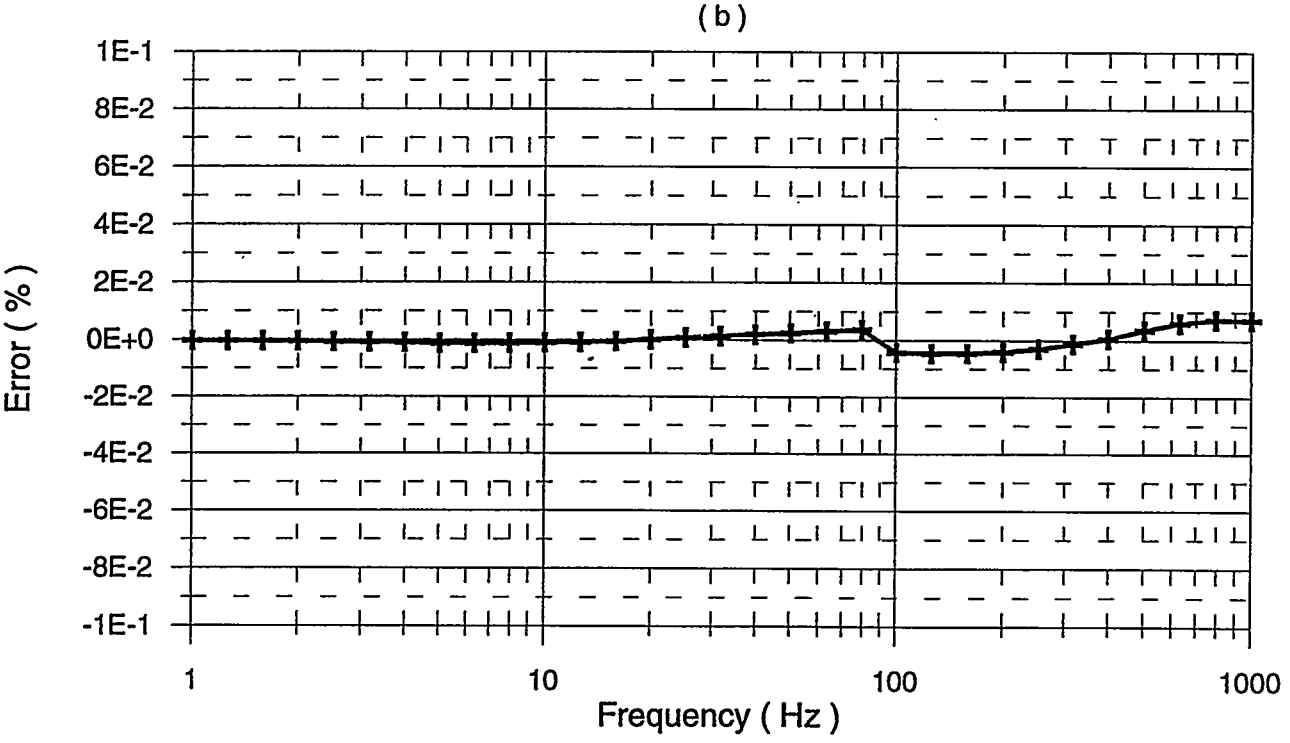

Figure 8. (a) Recovered Quadrature Formation Signal
(b) Error in Recovered Signal

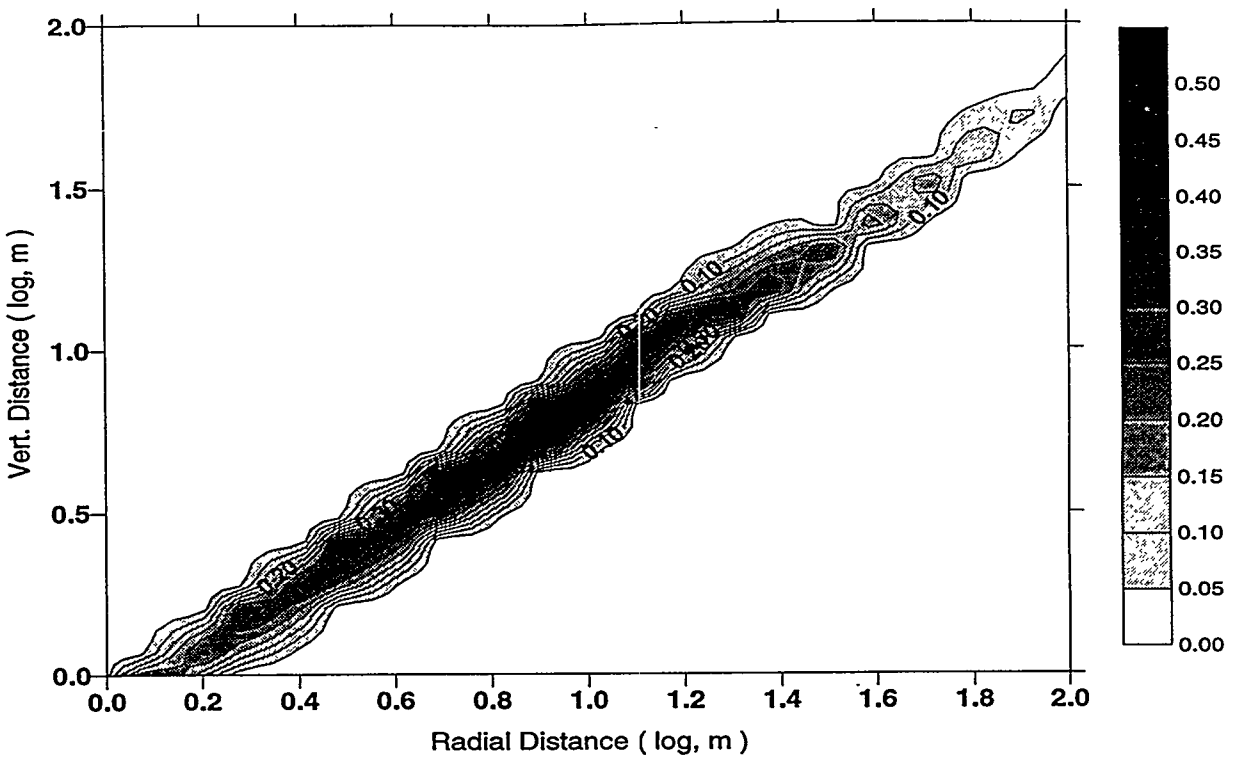

Figure 9. Percentage Amp. Difference at 300 Hz

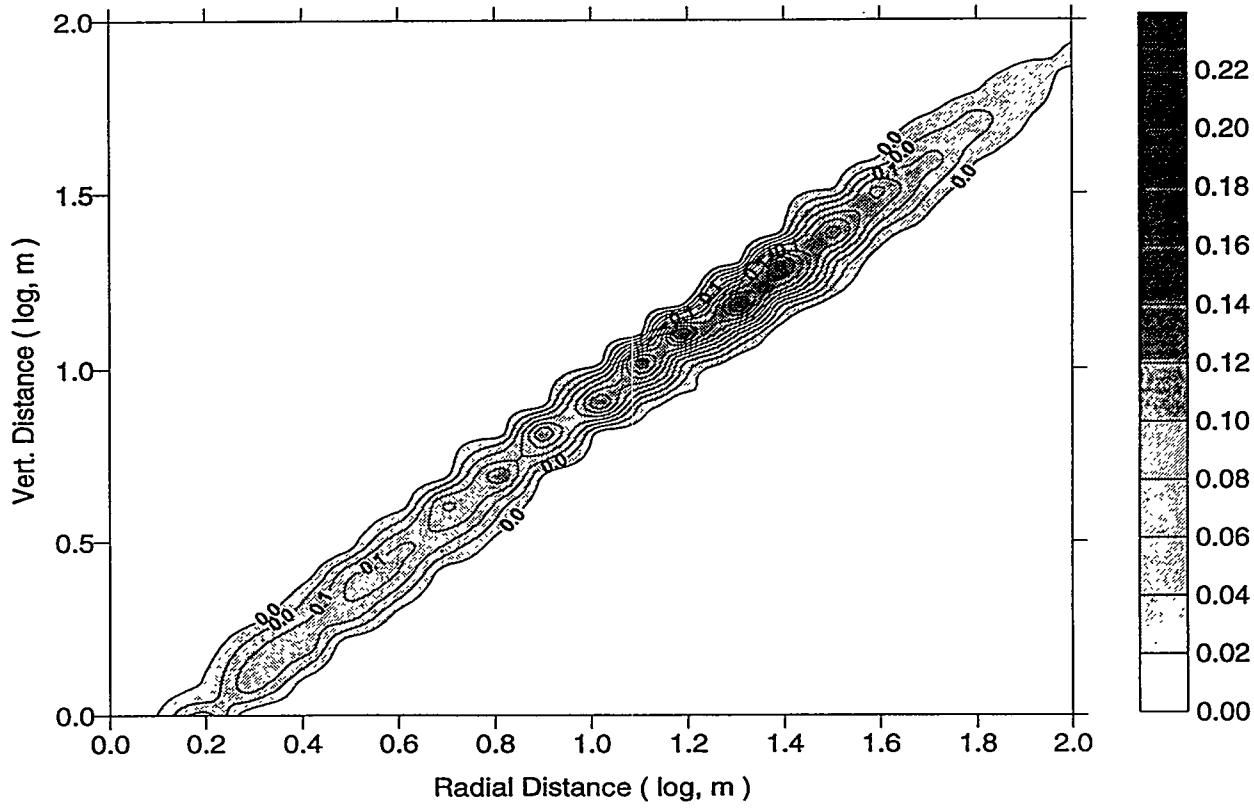

Figure 10. Difference in Phase at 300 Hz (degree)

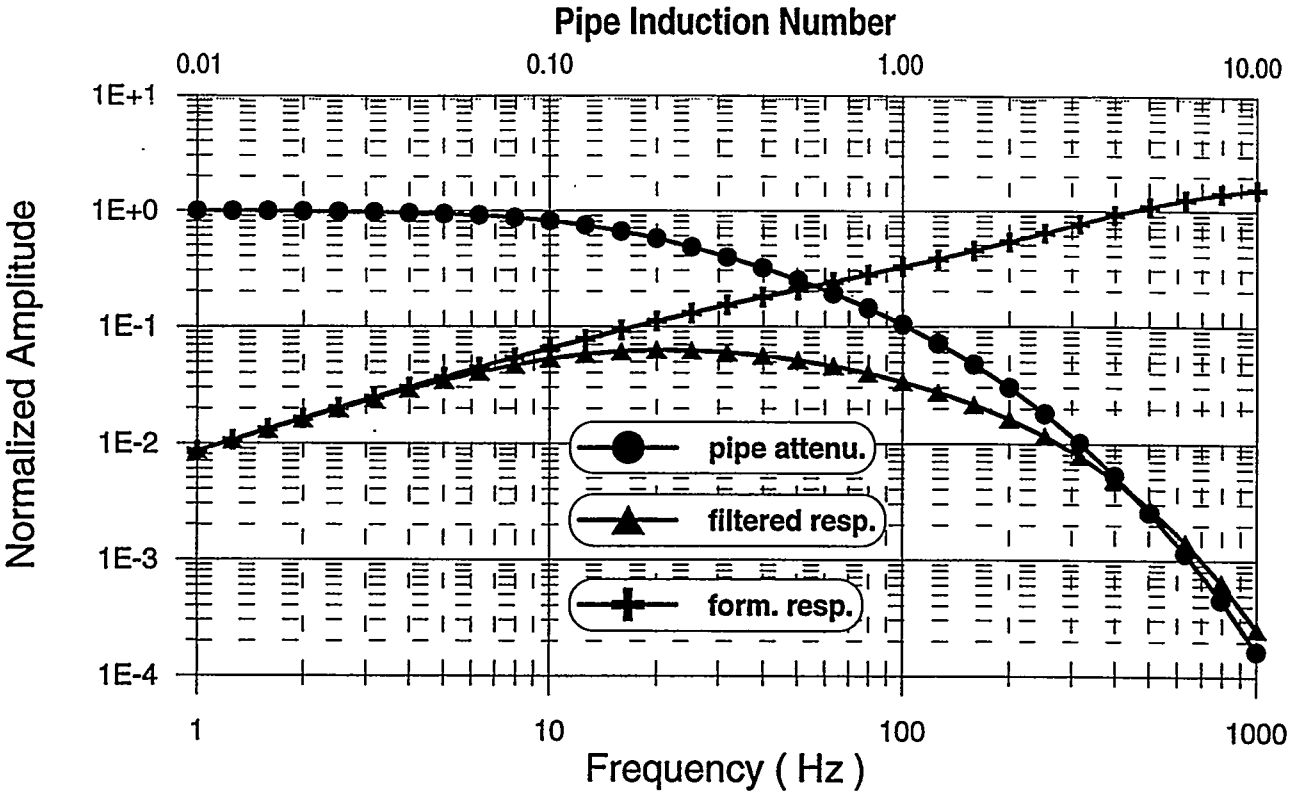

Figure 11. Filtered Formation Signal

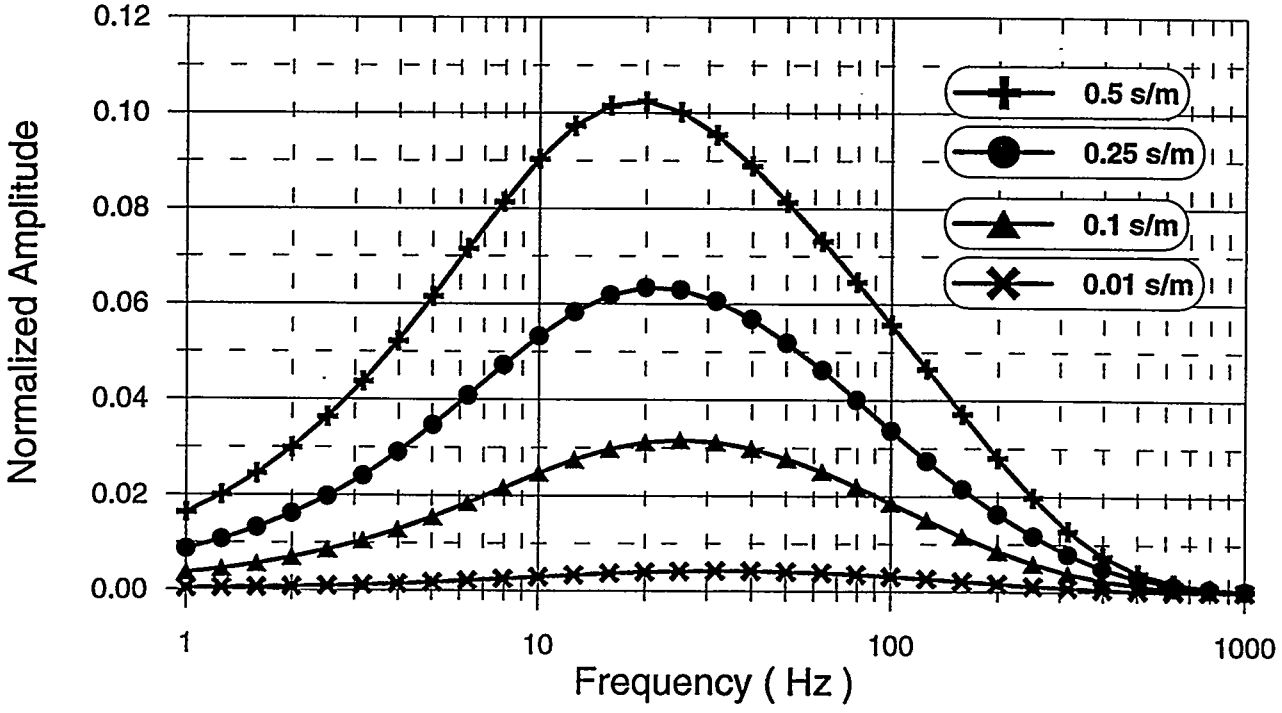

Figure 12. Optimal Response

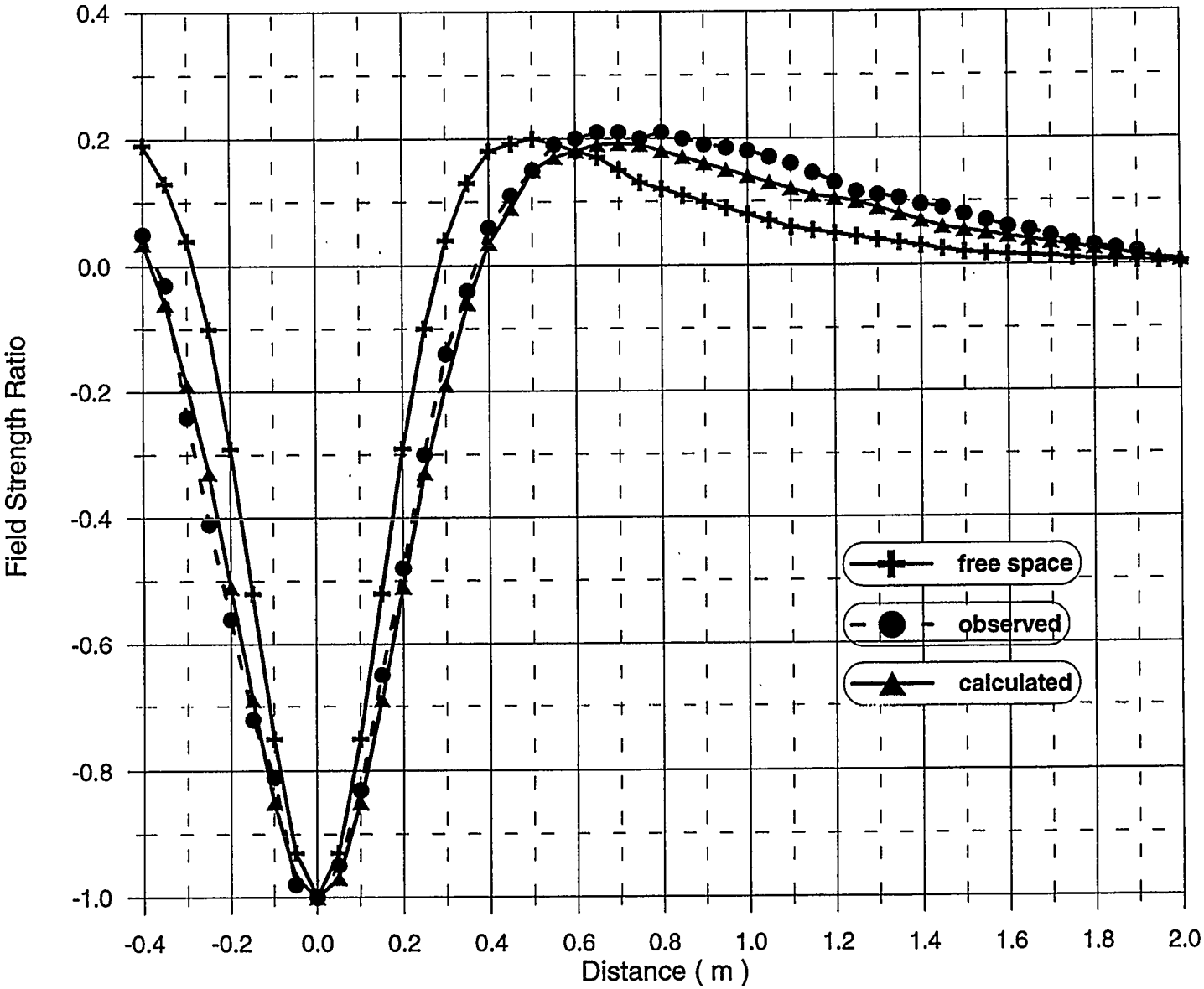

Figure 13. DC Profile at 40 cm Separation

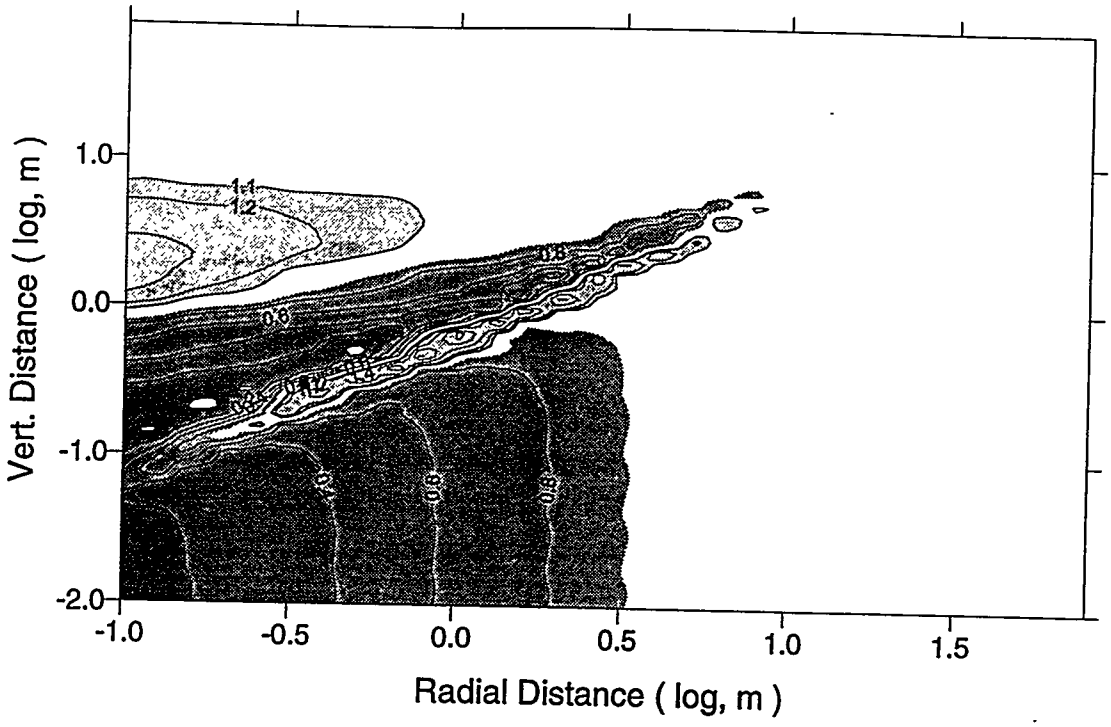

Figure 14. Bc/Bo, Normalized Magnetic Field Outside the Pipe

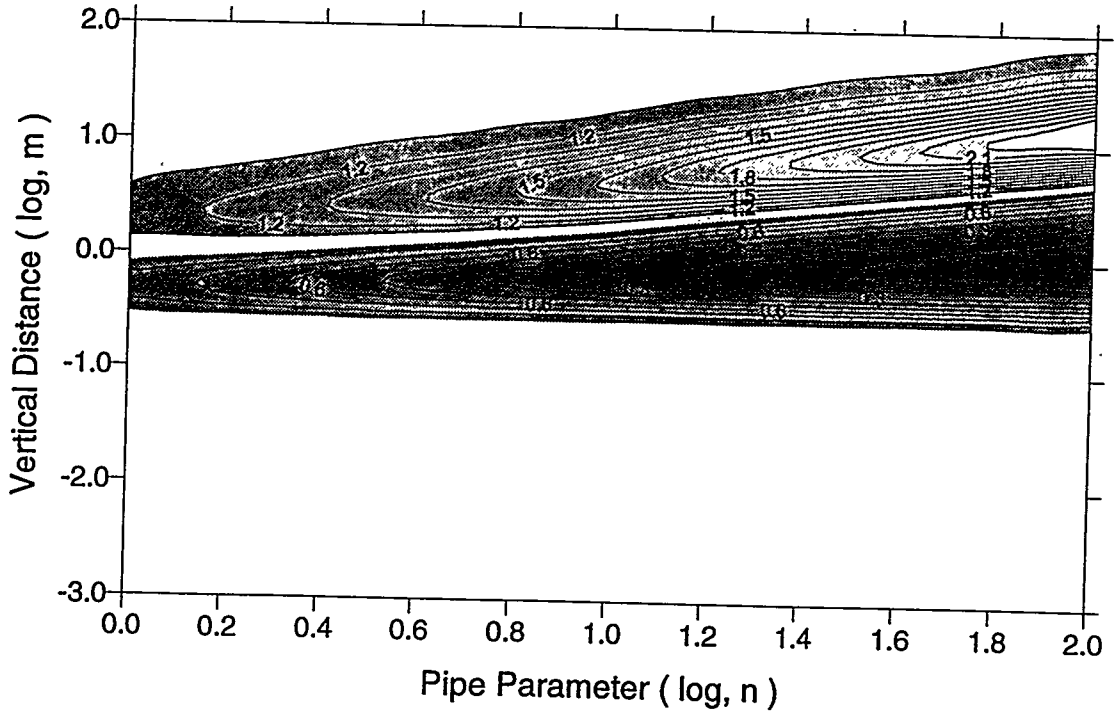

Figure 15. Bc/Bo, Normalized Magnetic Field Inside the Pipe